Influence of Al on the Microstructural Evolution and Mechanical Behavior of Low-Carbon, Manganese Transformation-Induced-Plasticity Steel

DONG-WOO SUH, SEONG-JUN PARK, TAE-HO LEE, CHANG-SEOK OH, and SUNG-JOON KIM

Microstructural design with an Al addition is suggested for low-carbon, manganese transformation-induced-plasticity (Mn TRIP) steel for application in the continuous-annealing process. With an Al content of 1 mass pct, the competition between the recrystallization of the cold-rolled microstructure and the austenite formation cannot be avoided during intercritical annealing, and the recrystallization of the deformed matrix does not proceed effectively. The addition of 3 mass pct Al, however, allows nearly complete recrystallization of the deformed microstructure by providing a dual-phase cold-rolled structure consisting of ferrite and martensite and by suppressing excessive austenite formation at a higher annealing temperature. An optimized annealing condition results in the room-temperature stability of the intercritical austenite in Mn TRIP steel containing 3 mass pct Al, permitting persistent transformation to martensite during tensile deformation. The alloy presents an excellent strength-ductility balance combining a tensile strength of approximately 1 GPa with a total elongation over 25 pct, which is comparable to that of Mn TRIP steel subjected to batch-type annealing.

DOI: 10.1007/s11661-009-0124-7

I. INTRODUCTION

TRANSFORMATION-INDUCED-PLASTICITY (TRIP) steel is a representative high-strength steel that utilizes phase transformation to control the mechanical properties.[1–5] Strain-induced martensitic transformation of metastable austenite plays a major role in improving the mechanical balance (tensile strength × elongation), allowing TRIP steel to be actively applied in the automotive industry. Currently, the tensile strength of commercially produced TRIP steel reaches approximately 1000 MPa. However, when the tensile strength exceeds 800 MPa, the elongation tends to decrease to less than 15 pct and the mechanical balance is significantly deteriorated.[6,7] Recently, Matlock *et al*. suggested a guideline for improving the mechanical balance of higher-strength multiphase steel, taking into account the characteristics of constituting phases.[8] They emphasized that a microstructural control ensuring higher stability as well as a sufficient fraction of austenite would be essential to obtaining a higher tensile strength with desirable elongation.

Low-carbon, manganese TRIP steel (Mn TRIP steel) based on an alloy system of Fe-0.1C-5Mn was first introduced by Miller.[9] A retained austenite fraction of 20 to ~40 pct with optimized stability made it possible to exhibit an excellent mechanical balance after intercritical annealing. However, a prolonged heat treatment using a batch-type annealing process was required to obtain the desired properties; thus, the more modern continuous-annealing conditions were not tested.[9–12] In the present study, we investigated the influence of Al on the microstructural evolution and mechanical behavior of Mn TRIP steel using the continuous-annealing process in order to obtain an exceptional mechanical balance. The Mn TRIP steels with different Al contents are prepared and heat treated under continuous-annealing conditions. The recrystallization of the cold-rolled structure consisting of martensite or ferrite and the formation of austenite during intercritical annealing are investigated, and the mechanical behavior of annealed sheets is examined with respect to the fraction and stability of retained austenite.

II. MICROSTRUCTURAL DESIGN USING AL ADDITION

The microstructure of conventional TRIP steel consists of polygonal ferrite, bainitic ferrite, and retained austenite. This microstructure is obtained by means of a two-step heat treatment that includes intercritical annealing and austempering. During the intercritical annealing, recrystallization of the cold-rolled microstructure and the reverse transformation to austenite occur. Epitaxial ferrite and bainitic ferrite start to form during rapid cooling and austempering, which enriches

DONG-WOO SUH, Associate Research Professor, is with the Graduate Institute of Ferrous Technology (GIFT), Pohang University of Science and Technology (POSTECH), Pohang, 790-784 Korea. Contact e-mail: dongwoo1@postech.ac.kr SEONG-JUN PARK and TAE-HO LEE, Senior Researchers, and CHANG-SEOK OH and SUNG-JOON KIM, Principal Researchers, are with the Structural Materials Division, Korea Institute of Materials Science, Changwon, Kyungnam, 641-010 Korea.

Manuscript submitted April 3, 2009.
Article published online December 3, 2009

the austenite with carbon and thereby establishes the thermal stability of the retained austenite during the final cooling to room temperature.[13] In conventional TRIP steels, the large uniform deformation resulting from the strain-induced martensitic transformation of austenite contributes to the improvement in the mechanical balance. The recrystallization of ferrite, however, is also important to obtaining a desirable mechanical balance, because the ferritic matrix phase is subjected to a considerable amount of strain during deformation.

Meanwhile, in Mn TRIP steel, the enhanced hardenability of intercritical austenite due to its higher Mn content makes it difficult to control the fraction and stability of the austenite by a subsequent heat treatment following the intercritical annealing. This implies that it is necessary to achieve the specific characteristics of the austenite in the course of the single-step heat treatment of intercritical annealing. The Mn additions substantially lower the temperature for the initiation of austenite formation during heating (A_s). Accordingly, when Mn TRIP steel is annealed at a sufficiently high temperature at which recrystallization can be completed in a short time, the fraction of reverse-transformed austenite drastically increases and it becomes difficult to achieve the required thermal stability of austenite during final cooling. To address this difficulty, annealing at a temperature below 650 °C was adopted in previous studies of Mn TRIP steels.[9–12] This approach permitted the control of the austenite fraction in the range of 20 to ~30 vol pct with a fine-grained structure. The prolonged annealing time (>1 hour) was required for the recrystallization of the cold-rolled microstructure and the partitioning of Mn between ferrite and austenite.[10–12]

During a typical continuous-annealing processing, the annealing temperature is generally higher than that of batch-type annealing, to complete the recrystallization of the cold-rolled structure during the rapid heating and short holding time. Controlling the fraction and stability of austenite formed at higher annealing temperatures will therefore be critical for the application of the continuous-annealing process to Mn TRIP steel. Figure 1 shows the equilibrium phase fractions in the Fe-0.12C-5Mn-0.5Si alloy system as a function of the Al content. The calculation is performed with the CALPHAD method[14] using a modified database that takes into account recent experimental results for the Fe-Mn-Al-C alloy system.[15] In the temperature range 700 °C to ~800 °C, in which the recrystallization of the cold-rolled structure is expected to occur actively, the calculated equilibrium fraction of austenite is 67 to ~100 pct in the case of the Al-free steel. The equilibrium fraction of austenite gradually falls off as the Al content increases and it is found that the single-austenite-phase region disappears and that the equilibrium fraction of austenite can be reduced to 20 to ~30 pct with the addition of 3 mass pct Al. This represents that Al will suppress the excessive formation of austenite even at the higher temperature applicable for the continuous annealing of Mn TRIP steel. This also has a favorable effect on the stability of intercritical austenite. The influence of Al on the equilibrium phase fraction suggests that a microstructure design with Al might be one of the ways to manipulate the characteristics of intercritical austenite in Mn TRIP steel. The microstructural control by the Al addition is verified with the experimental procedures in Section III.

III. EXPERIMENTAL

Table I shows the chemical compositions of the investigated alloys. Based on the Al-free Fe-0.12C-5Mn-0.5Si alloy system, L-Al (1 mass pct Al) and H-Al (3 mass pct Al) alloys were prepared. Vacuum-induction-melted ingots with dimensions of 300 × 150 × 50 mm were reheated to 1200 °C for 2 hours and hot rolled with a finishing temperature above 800 °C, followed by air cooling to room temperature. The thickness of the hot-rolled sheets was 4.5 mm. They were pickled in a 10 pct HCl solution and then cold rolled to a thickness of 1 mm. The cold-rolled sheets were annealed using an infrared heating furnace, with heating and cooling rates of 10 °C/s. The intercritical annealing temperatures of 660 °C, 720 °C, and 780 °C for the L-Al alloy and 720 °C, 780 °C, 840 °C for the H-Al alloy were chosen, taking into account the calculated equilibrium austenite fraction. The holding time at each annealing temperature was 2 minutes. Light microscopic observation was performed with a standard method using a 2 pct nital solution. For microstructural characterization using a scanning electron microscope equipped with an electron backscattered diffraction (EBSD) attachment, the specimens were mechanically polished with a colloidal silica suspension in the final polishing stage. The step size for the EBSD measurement was 0.05 or 0.025 μm, depending on the scale of microstructure. Thin foils for the transmission electron microscope (TEM) were chemically polished in a 10 pct $HF + H_2O_2$ solution to a thickness of 50 μm and then electrolytically polished in a twin-jet polishing apparatus using a solution containing 15 pct $HCHO_4 + CH_3OH$ at −20 °C. The fraction of retained austenite was determined by XRD using Cu K_α radiation. Specimens were prepared by mechanical polishing followed by chemical polishing in a 10 pct $HF + H_2O_2$ solution. Integrated intensities of $(200)_\alpha$, $(211)_\alpha$, and $(220)_\gamma$, $(311)_\gamma$ reflections were used for the determination of the phase fraction of austenite.[16] The uncertainty of the austenite fraction with the XRD analysis is known to be approximately 5 pct of the evaluated one. It will be enlarged when the specimen has a preferred orientation, which is not considered in the present study.[17] The mechanical properties of the annealed sheets were examined with a universal tensile testing machine, using a crosshead speed of 2 mm/min. Subsized test coupons according to the ASTM[18] were used for the tensile tests.

IV. RESULTS

A. *Microstructural Evolution*

Figure 2 shows the microstructures of the hot-rolled sheets. The microstructure of the L-Al alloy consists

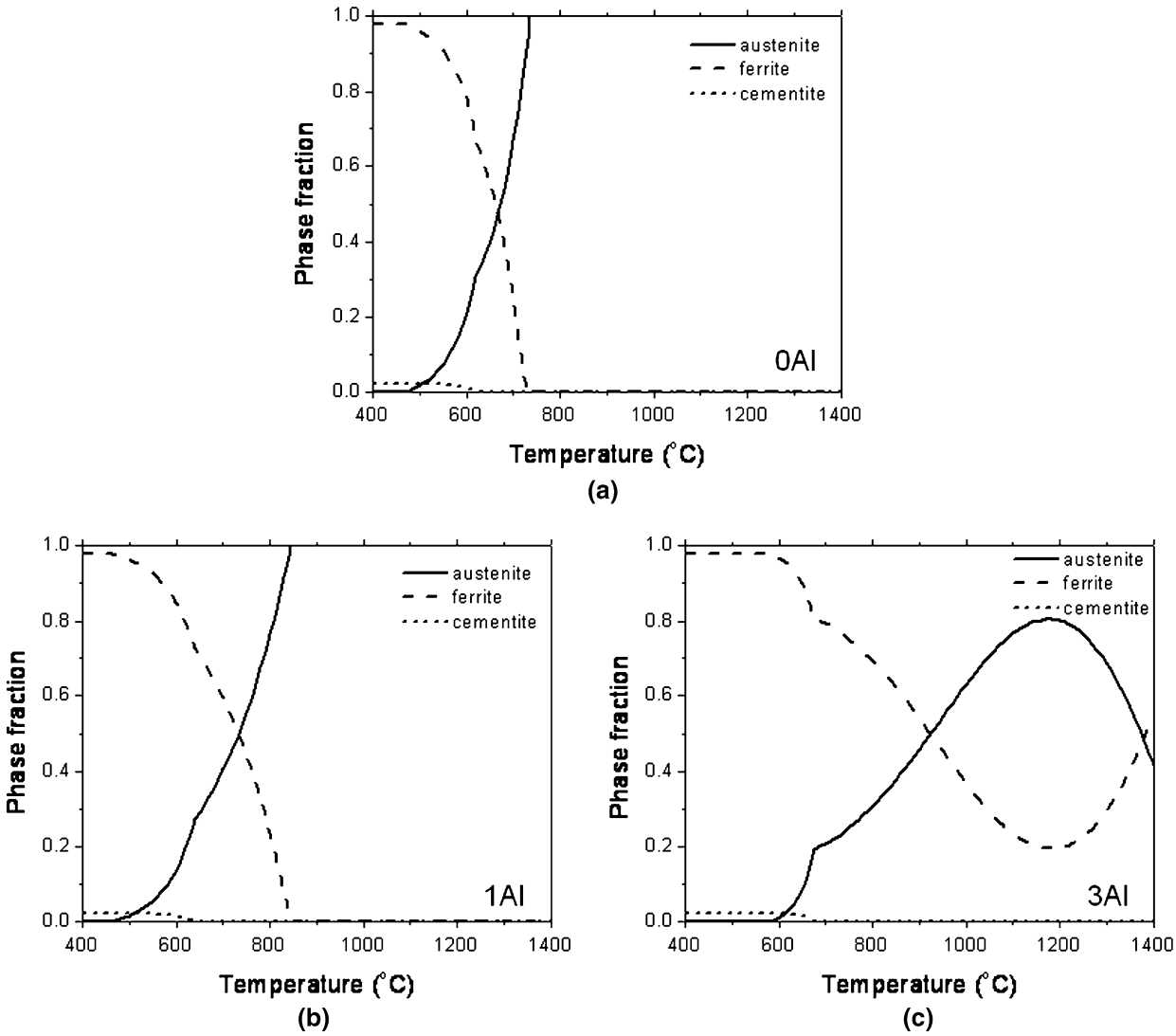

Fig. 1—Equilibrium fraction of constituting phases in Fe-0.12C-5Mn-0.5Si alloy system containing (*a*) 0 mass pct Al, (*b*) 1 mass pct Al, and (*c*) 3 mass pct Al.

Table I. Chemical Compositions of Investigated Alloys (Mass Percent)

	C	Mn	Si	Al
L-Al	0.12	4.6	0.55	1.1
H-Al	0.12	5.8	0.47	3.1

largely of martensite. It also contains a small fraction of white grains, indicated with arrows, which are presumed to be ferrite. The microstructure mainly covered with martensite is ascribed to the high Mn content, which considerably increases the hardenability of the alloy. For the H-Al alloy, the hot-rolled structure is a mixture of elongated ferrite and martensite. Given that the hot rolling was conducted in the temperature range 800 °C to ~1200 °C, the calculated phase fraction in Figure 1(c) implies that the microstructure consists of austenite and ferrite during the hot rolling, which results in the elongated structure of ferrite and martensite after cooling. For steels with a high Mn content, Mn segregation frequently occurs and has an influence on the microstructural evolution.[19] The Mn segregation possibly developed in the investigated alloys. In the banded structure of the ferrite and martensite of the H-Al steel, the ferrite and martensite will correspond to the Mn lean and rich regions, respectively, because Mn is an austenite stabilizer and, therefore, the ferrite will preferentially form in a Mn-lean region. The energy dispersive spectroscopy (EDS) analysis shows that the Mn content in ferrite is 5.5 ± 0.2 mass pct and in martensite is 6.9 ± 0.2 mass pct, which confirms the nonuniform distribution of Mn. The Mn segregation will affect the microstructural evolution during the subsequent process, which will be discussed later in this article.

Figures 3 and 4 give the microstructures of annealed sheets after cold rolling, observed with a light microscope. Recrystallized polygonal ferrite grains are hardly found in the L-Al alloy for any annealing condition. Recovery is supposed to occur in the cold-rolled

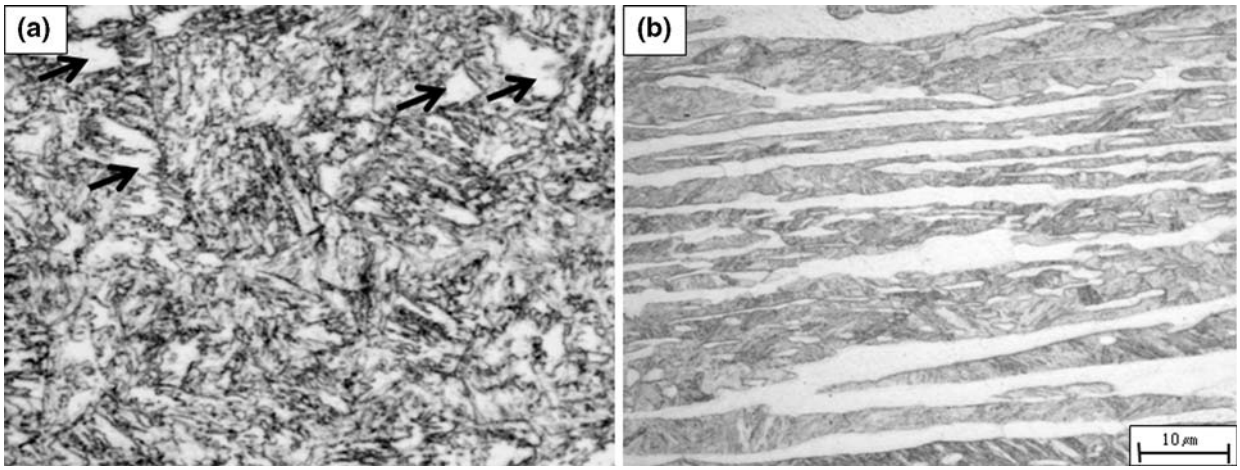

Fig. 2—Optical micrographs of hot-rolled sheets for (*a*) L-Al and (*b*) H-Al alloys.

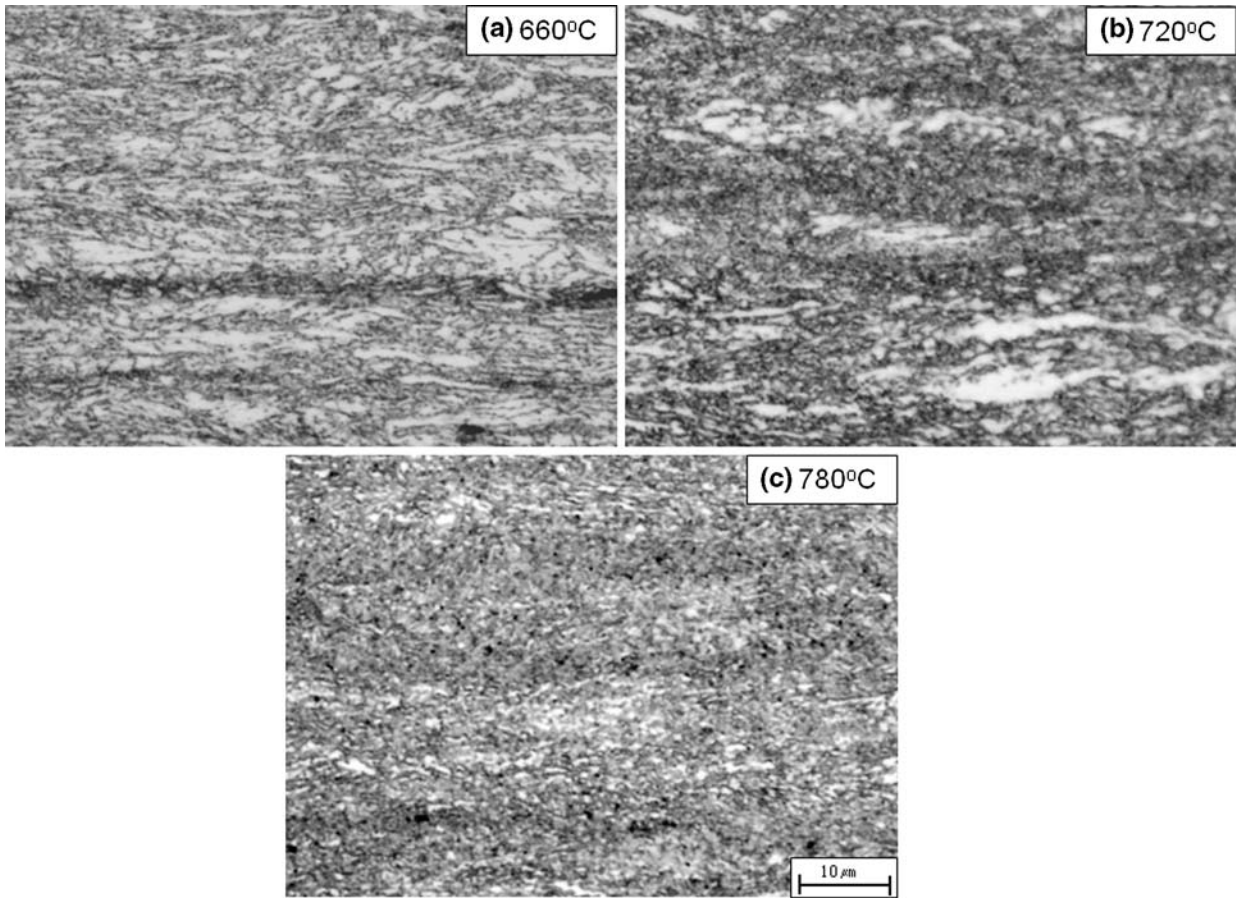

Fig. 3—Optical micrographs of cold-rolled L-Al alloy after annealing for 120 s at (*a*) 660 °C, (*b*) 720 °C, and (*c*) 780 °C.

structure as an increase in the annealing temperature, but it is not likely to proceed actively at an annealing temperature of 780 °C. It is believed to be related to the retransformation of austenite into fresh martensite during cooling from an intercritical temperature. Meanwhile, recrystallized grains are observed in the H-Al alloy for all annealing conditions. When annealed at 720 °C, recrystallization takes place in coarse ferrite (A), and fine grains presumed to be reverse-transformed austenite are observed in regions that were formerly martensite (B). It is noted that austenite grains evolve preferentially in a Mn-rich region. An increase in the

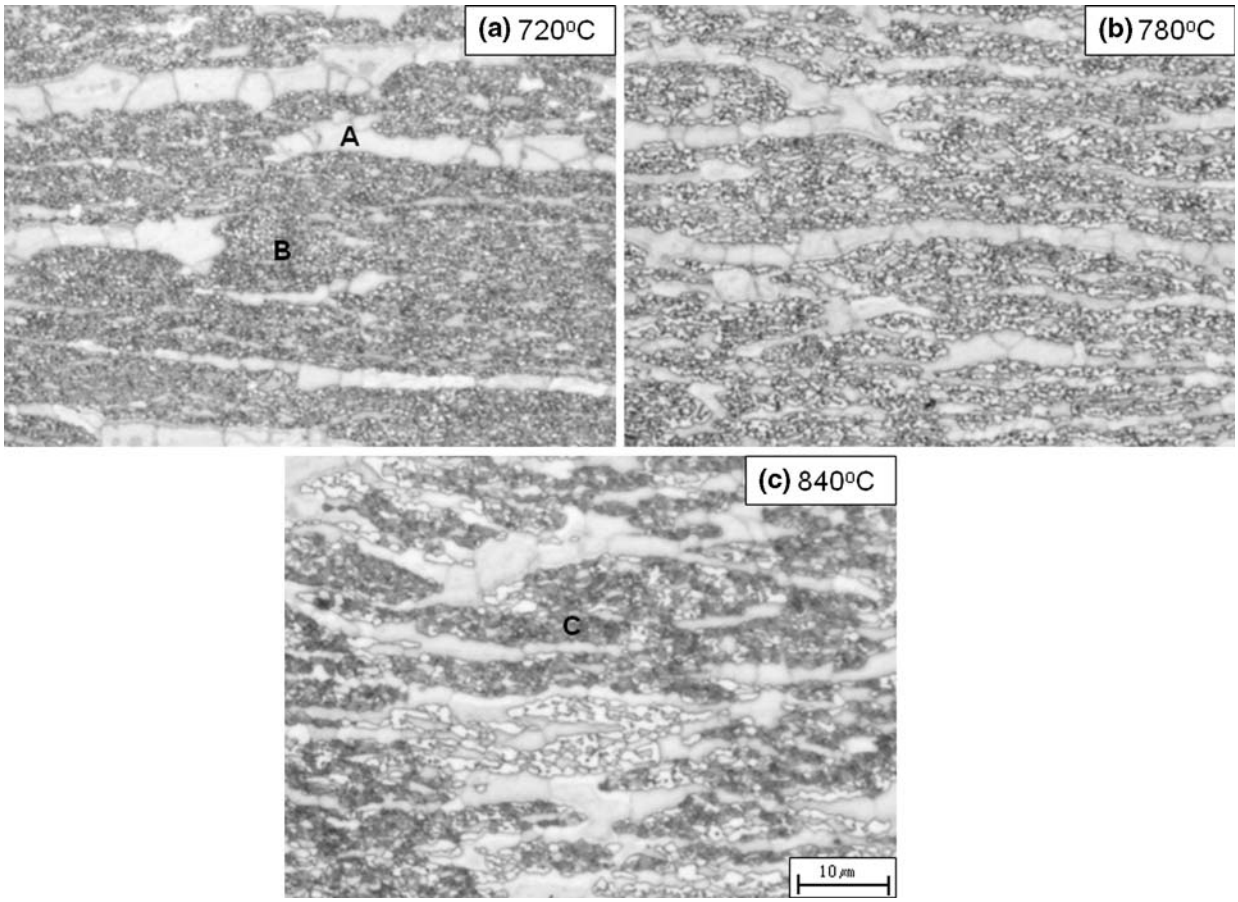

Fig. 4—Optical micrographs of cold-rolled H-Al alloy after annealing for 120 s at (*a*) 720 °C, (*b*) 780 °C, and (*c*) 840 °C.

annealing temperature to 780 °C clarifies the newly transformed austenite grains, but a further increase in the annealing temperature to 840 °C introduces another phase (C), which is thought to be fresh martensite transformed from the intercritical austenite upon cooling.

Figure 5 shows the retained austenite fraction in annealed sheets evaluated from XRD profiles. In the L-Al alloy, the retained austenite fraction is 6 pct after annealing at 660 °C. It is considerably increased to 28 pct after annealing at 720 °C, and then is decreased to 6 pct when annealed at 780 °C. The retained austenite fraction in the H-Al alloy can be preserved at approximately 26 to ~31 pct after annealing at temperatures of 720 °C and 780 °C, but it drops to 18 pct after annealing at 840 °C. Together with the microstructural observation, the dilatometric curves in Figure 6 indicate that the change in the retained austenite fraction with the annealing temperature is associated with the martensite transformation. When martensite forms from austenite during cooling, the dilatometric curve deviates from the linear behavior due to the atomic volume difference between martensite and austenite.[20] The onset of deviation indicates the M_s temperature, as shown by the arrow. The dilatometric curves in Figure 6 reveal that the intercritical austenite is stable enough to resist martensite formation on cooling when annealed at

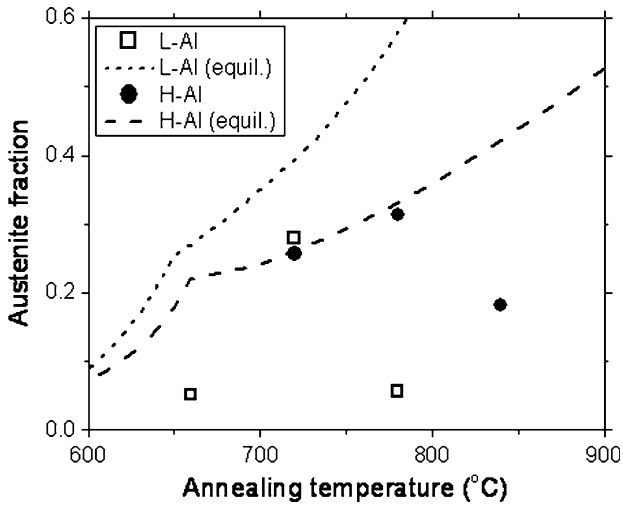

Fig. 5—Fraction of austenite retained after intercritical annealing (Broken lines are equilibrium fraction and symbols are measured ones from XRD profiles).

680 °C and720 °C for the L-Al alloy and 720 °C and 780 °C for the H-Al alloy, but additional increments in the annealing temperature lead to martensite formation in both alloys. The deterioration in the thermal stability

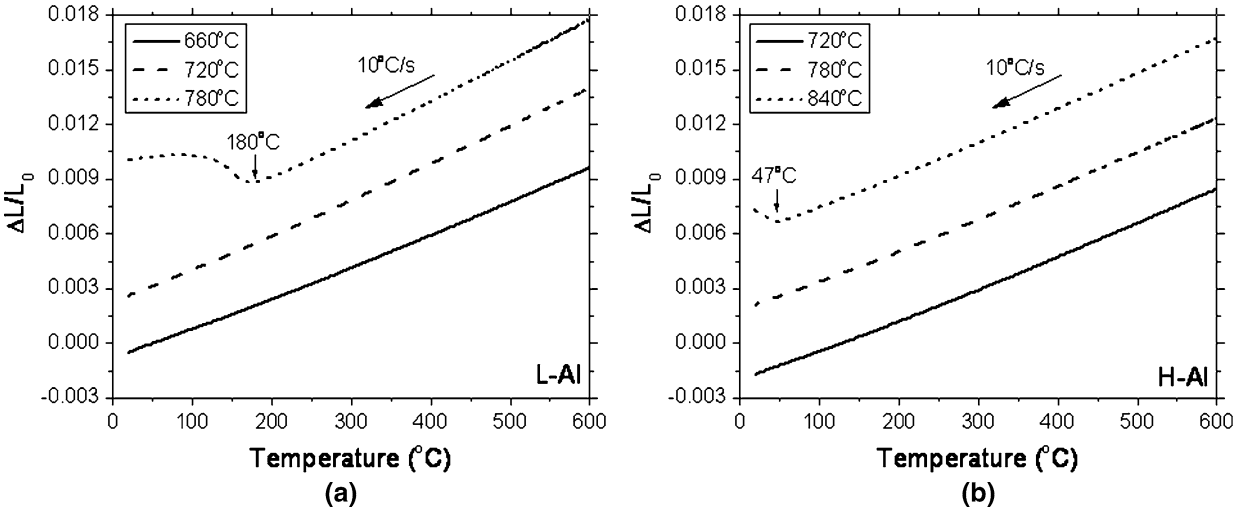

Fig. 6—Dilatometric curves upon cooling for intercritically annealed (*a*) L-Al and (*b*) H-Al alloys.

of intercritical austenite is believed to be connected with a lowering of the carbon content and a coarsening of the austenite grains accompanied by a rapid increase in the austenite fraction during the annealing at a higher temperature. The more remarkable decrease in the austenite fraction in the L-Al alloy having a larger equilibrium austenite fraction at the annealing temperature implies that the thermal stability of the intercritical austenite is closely related to the fraction of austenite formed during annealing.

For detailed microstructure observations, EBSD analysis was performed on specimens containing comparable volume fractions of austenite after the heat treatment. The L-Al alloy annealed at 720 °C and the H-Al alloy annealed at 720 °C and 780 °C have austenite fractions of 0.28, 0.26, and 0.31, respectively. Figure 7 shows the phase mappings with boundary characteristics. In the L-Al alloy, fine austenite grains (fcc) reverse transformed during annealing can be distinguished. A considerable fraction of low-angle boundaries in the region indexed as bcc suggests that the recrystallization does not proceed effectively.[21,22] In contrast, the H-Al alloy exhibits completely recrystallized coarse ferrite grains with primarily high-angle boundaries. Small ferrite grains are also found in the region in which fine austenite grains are formed. Some of them contain low-angle boundaries, which indicates that the recrystallization is not completed in this region, but the overall microstructure indicates that the recrystallization of the cold-rolled microstructure is nearly completed. The dissimilar restoration processes of the cold-rolled structure in the L-Al and H-Al alloys lead to different boundary characteristics in the annealed sheets. The distribution of the misorientation angles in Figure 8 shows that 77.5 pct of the boundaries in the L-Al alloy are low-angle boundaries ($0.5 < \theta < 15$ deg). The fraction of low-angle boundaries is only 43.8 pct in the H-Al alloy annealed at 720 °C and decreases further to 39.4 pct when it is annealed at 780 °C. A larger fraction of low-angle boundaries denotes a residual deformed microstructure and thus a sluggish progress of the recrystallization during annealing. The distribution of the equivalent grain diameter of austenite and ferrite is presented in Figure 9 and the average grain diameter is summarized in Table III. The reverse-transformed austenite grain has a finer average diameter than ferrite grain, as expected from the microstructural observation. It is noted that even though a few ferrite grains have a grain size of approximately 5 μm, the average diameter of the ferrite grain is still evaluated to be submicron scale. That is because the average diameter is the arithmetic mean, not considering the area occupied by each grain. That is also the reason that the duplex grain structure, consisting of coarse and fine ferrite grains in the H-Al alloy, is not clearly seen in the grain diameter distribution in Figure 9.

Figure 10 shows the TEM micrographs and EDS analysis results for the Mn content of some austenite grains in the annealed sheets. The deformed structure on the right side of Figure 10(a) and the dislocation substructures in the polygonal ferrite grains consistently indicate that the recrystallization occurs in a sluggish manner in the L-Al alloy. In contrast, the equiaxed grains with few dislocations suggest a nearly complete recrystallization in the H-Al alloy. The average Mn content of 15 austenite grains is 6.2 ± 0.8 mass pct in the L-Al alloy and 7.2 ± 0.4 mass pct for 24 austenite grains in the H-Al alloy. Table II compares the nominal Mn content in the alloys, the calculated equilibrium Mn content at each annealing temperature, and the measured ones. The Mn contents in austenite do not reach levels that correspond to full partitioning. Furthermore, as mentioned earlier, the Mn content in the Mn-segregated region reaches 6.9 mass pct in the H-Al alloy before annealing. It means that the redistribution of Mn during intercritical annealing is not so appreciable, which may come from the short annealing time.

B. *Mechanical Behavior*

The average tensile properties of the annealed sheets are summarized in Table IV, and representative

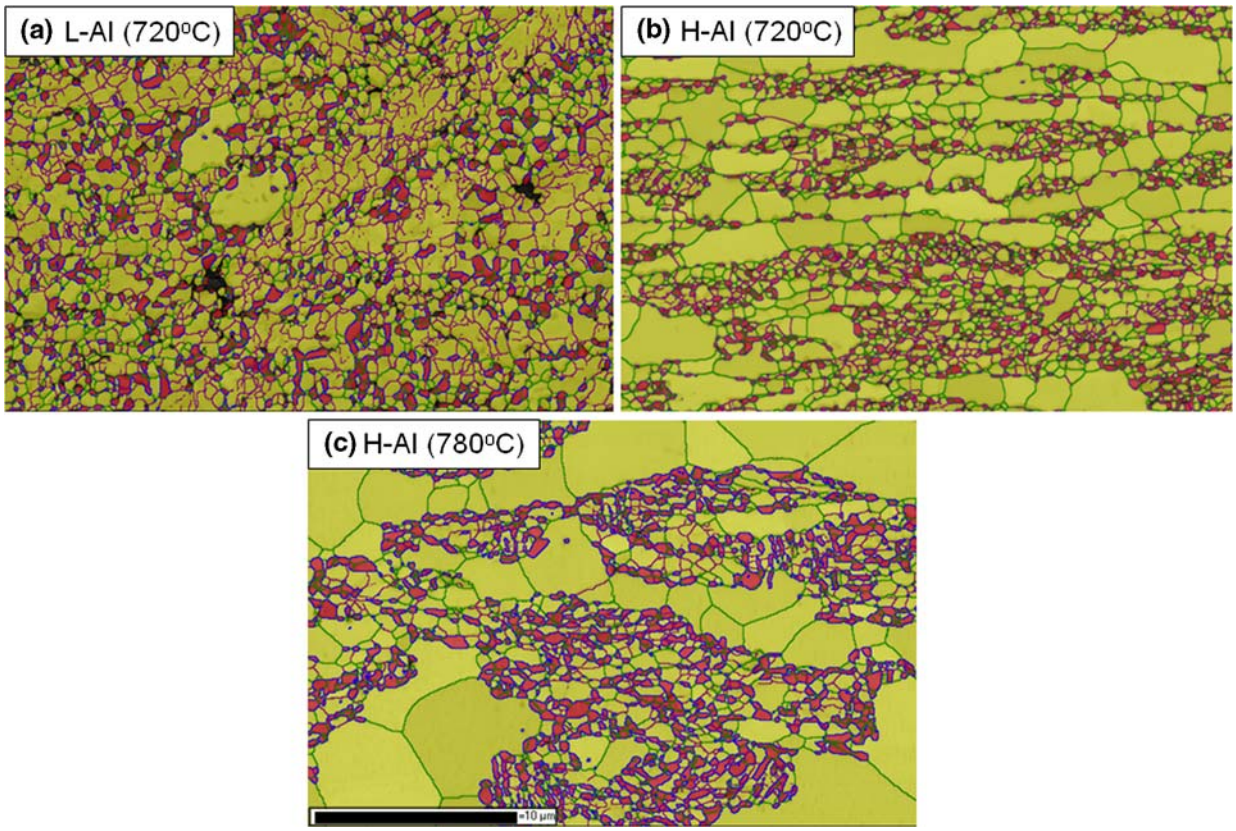

Fig. 7—EBSD phase mapping of (*a*) L-Al alloy annealed at 720 °C, (*b*) H-Al alloy at 720 °C, and (*c*) H-Al alloy at 780 °C, with indexing yellow phase as bcc and red phase as fcc (Misorientation is between 2 to ~15 deg for purple line and more than 15 deg for green line. Color image is available in the online article).

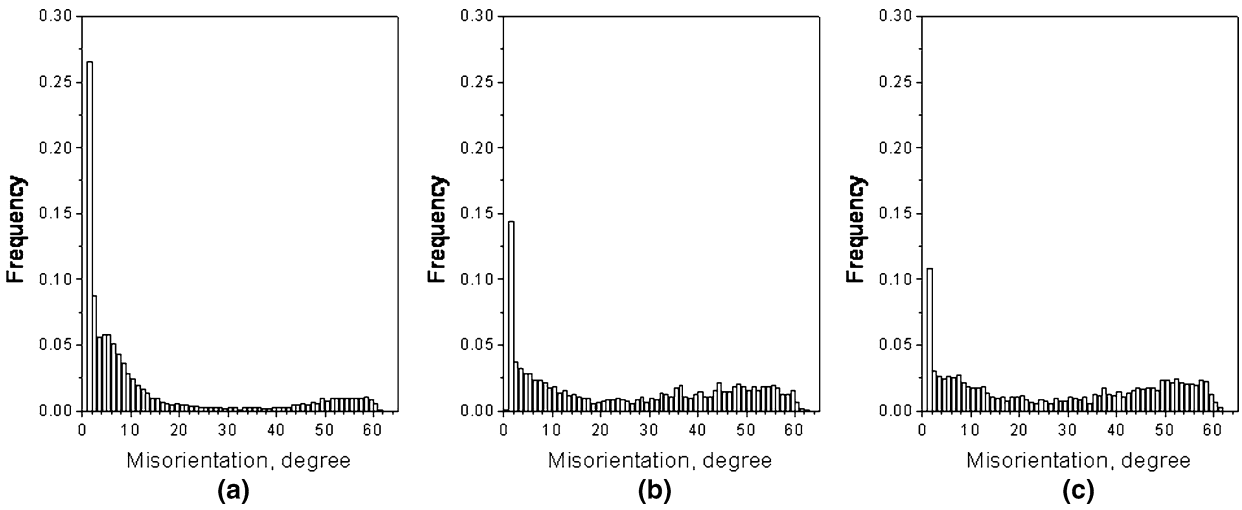

Fig. 8—Distribution of misorientation angle in (*a*) L-Al alloy annealed at 720 °C, (*b*) H-Al alloy at 720 °C, and (*c*) H-Al alloy at 780 °C.

stress-strain curves are shown in Figure 11. In the L-Al alloy, the tensile strength is improved by the increase in the annealing temperature, but the yield strength has a minimum value at the annealing temperature of 720 °C. After annealing at 660 °C and 720 °C, the microstructure consists of annealed martensite as the matrix phase and reverse-transformed austenite. Therefore, the yield strength will gradually decrease with an increase in annealing temperature due to the softening of the matrix phase. However, after annealing at 780 °C, a considerable amount of fresh martensite forms during cooling from the intercritical temperature, as indicated in the

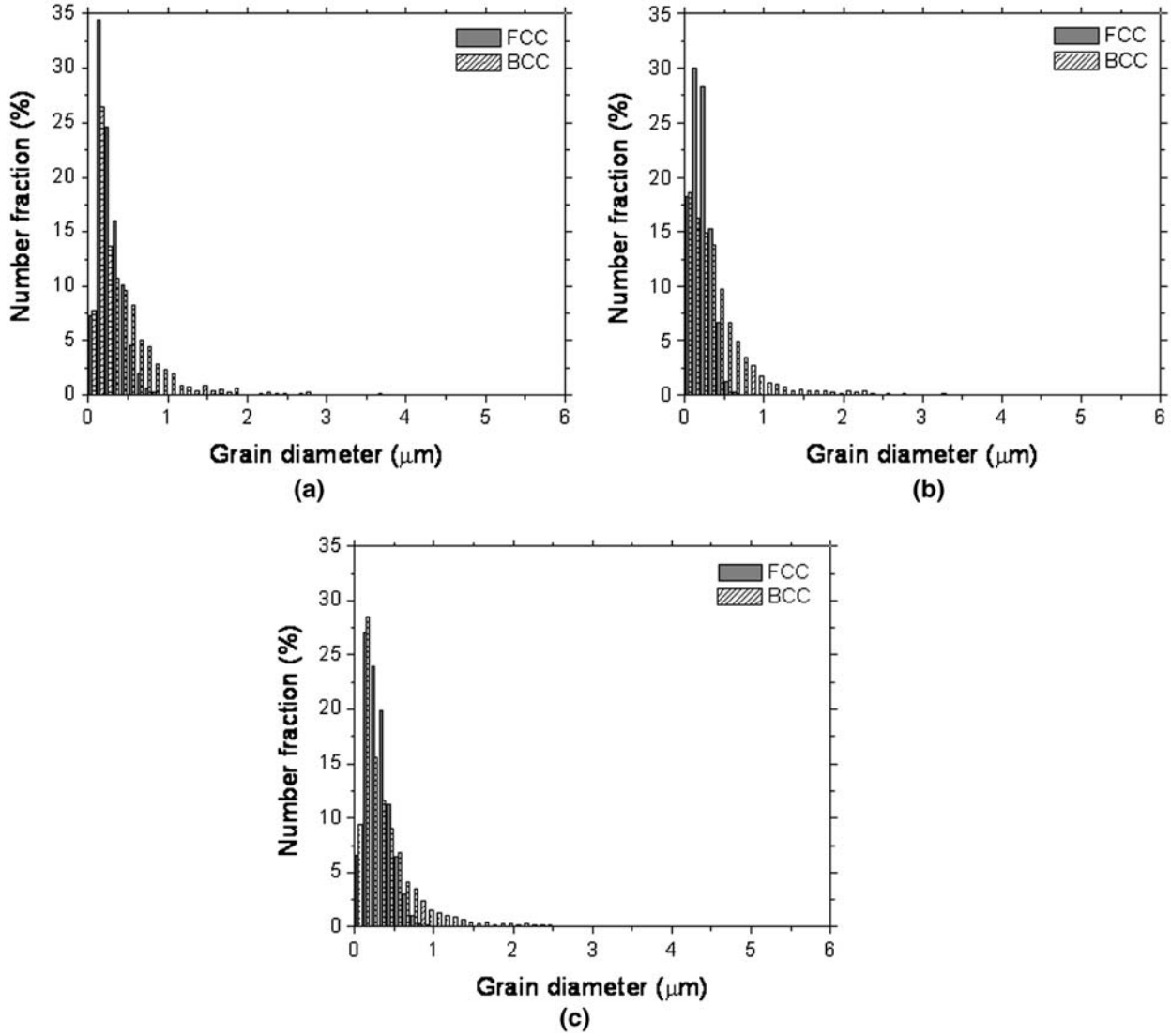

Fig. 9—Equivalent grain diameter distribution of ferrite and austenite in (*a*) L-Al alloy annealed at 720 °C, (*b*) H-Al alloy at 720 °C, and (*c*) H-Al alloy at 780 °C.

Table II. Mn Content in Austenitic Phase (Mass Percent)

	Nominal	Equilibrium Content at Annealing Temperature	Average of Measured Content
L-Al	4.6	7.6 (720 °C)	6.2
H-Al	5.8	8.8 (780 °C)	7.2

Table III. Average Equivalent Diameters of Austenite and Ferrite Grain from EBSD Analysis (Micrometers)

	L-Al (720 °C)	H-Al (720 °C)	H-Al (780 °C)
Austenite	0.26	0.22	0.29
Ferrite	0.47	0.42	0.43

dilatometric curve in Figure 6(a), and it contributes to the rebound in the yield strength. Meanwhile, the tensile strength is not only influenced by the yielding but is also affected by the work hardening, which reflects the microstructural evolution during deformation. For the L-Al alloy, the increase in the annealing temperature from 660 °C to 720 °C remarkably changes the work-hardening behavior. The notable work hardening obtained after annealing at 720 °C is very likely due to the increase in the austenite fraction shown in Figure 5. This contributes to the improvement in the tensile strength by strain-induced transformation to martensite. The tensile behavior of the specimen annealed at 780 °C does not exhibit a yield elongation but shows a rapid work hardening with the highest tensile strength. It is analogous to that of commercial dual-phase steel. Given that the considerable amount of martensite forms upon final cooling in that annealing condition, a high density of mobile dislocations is introduced to accommodate the volume expansion around the martensite. This accounts for the disappearance of the yield point elongation.[20]

A similar tensile behavior is observed for the H-Al alloy annealed at 840 °C, which also allows martensite formation on final cooling. In the H-Al alloy, the yield strength decreases with the increase in the annealing temperature. The major microstructural constituent is recrystallized ferrite after annealing of the H-Al alloy. The additional softening of ferrite with an increase in the annealing temperature is possibly associated with the change in the yield strength. The H-Al alloy annealed at 720 °C does not show a notable work hardening. Because the martensite formation has a primary effect on the work hardening of steels containing the retained austenite, the little work hardening, even with an austenite fraction of 26 pct before deformation, implies that the austenite is not likely to transform to martensite during the tensile test. Meanwhile, the tensile behavior of the H-Al alloy annealed at 780 °C is noteworthy, because the mechanical balance is remarkably improved compared with those annealed in different conditions. Due to a persistent work hardening along the deformation, it presents a higher tensile strength than that annealed at 720 °C even with a lower yield strength. This is a characteristic feature of TRIP steel with austenite having proper mechanical stability. The tensile strength of approximately 1 GPa with total elongation over 25 pct is comparable to those reported in 0.1C-5Mn alloys subjected to a batch-type annealing.[10–12] It confirms that low-carbon, manganese TRIP steel can be applied to the continuous-annealing process while maintaining the mechanical balance by microstructural control through an Al addition.

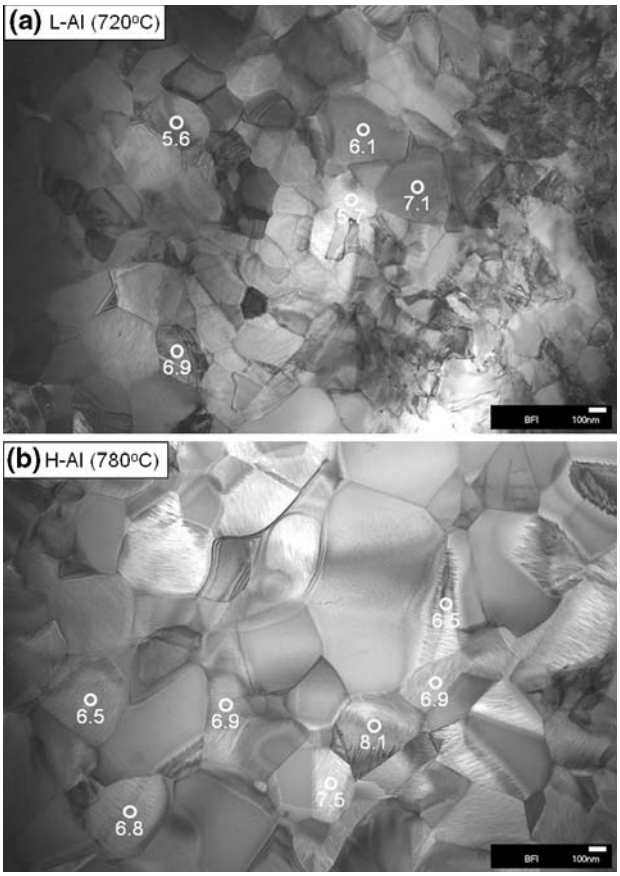

Fig. 10—TEM micrographs of (*a*) L-Al alloy annealed at 720 °C and (*b*) H-Al alloy at 780 °C with Mn content in austenite grain.

V. DISCUSSION

An addition of 3 pct Al to low-carbon, manganese TRIP steel permits both the recrystallization of the cold-rolled microstructure as well as the thermal stabilization of austenite during typical continuous-annealing processing. The alloy exhibits an excellent mechanical balance. The change in the retained austenite fraction according to the Al content and annealing temperature shows that, as intended in microstructure design using Al, the austenite stability can be secured by suppressing excessive austenite formation at a higher annealing temperature at which the recrystallization of the deformed microstructure is completed in a short time.

As mentioned, the recrystallization behavior of the cold-rolled structure is significantly influenced by the Al content. The recrystallized ferrite grains are rarely seen in the annealed L-Al alloy when observed by light microscopy and EBSD phase mapping. In addition, the polygonal ferrite grains found in the TEM micrographs are frequently observed to have dislocation substructures. In contrast, the coarse and fine ferrite grains in the annealed H-Al alloy have an equiaxed morphology and contain few dislocations. This reflects that the recrystallization in the H-Al alloy is almost completed, even at the same annealing temperature. The difference in the recrystallization behavior is thought to be attributed to the reduced competition between the recrystallization of the cold-rolled microstructure and the reverse transformation to austenite as a result of the higher Al content. In the L-Al alloy, the austenite fraction is approximately 30 pct at an annealing

Table IV. Average Tensile Properties of Investigated Alloys

		Yield Strength (MPa)	Tensile Strength (MPa)	Uniform Elongation (Pct)	Total Elongation (Pct)
L-Al	660 °C	936 ± 1.9	988 ± 2.9	11.5 ± 0.6	16.7 ± 1.7
	720 °C	766 ± 2.9	1204 ± 10.0	12.9 ± 0.3	15.9 ± 0.8
	780 °C	940 ± 2.6	1461 ± 6.4	6.2 ± 0.2	8.6 ± 1.3
H-Al	720 °C	814 ± 4.3	854 ± 2.5	14.7 ± 1.2	21.7 ± 3.9
	780 °C	714 ± 13.3	994 ± 10.4	23.8 ± 0.8	27.5 ± 1.1
	840 °C	444 ± 3.7	1161 ± 12.1	11.2 ± 0.2	12.4 ± 0.2

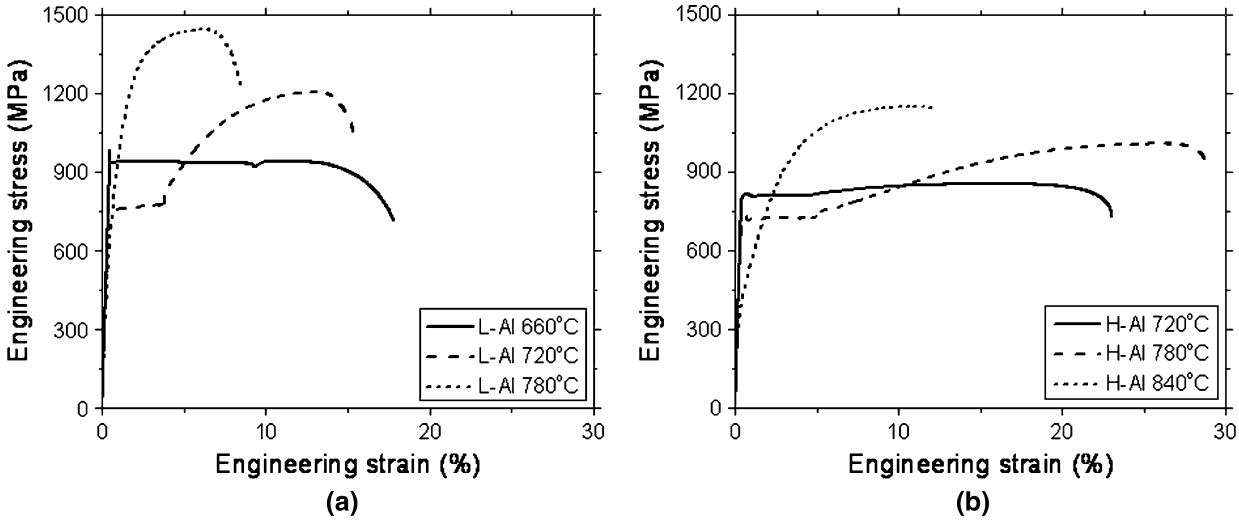

Fig. 11—Stress-strain curves of annealed sheets of (*a*) L-Al and (*b*) H-Al alloys.

temperature of 720 °C and it will increase rapidly at higher annealing temperatures. It means that the recrystallization of the deformed microstructure and the austenite formation proceed simultaneously during the intercritical annealing. Generally, the driving force for phase transformation is larger than that for recrystallization. From the calculation with the CALPHAD method using Thermo-Calc software (Thermo-calc software AB, Stockholm, Sweden),[14] the overall driving force for austenite formation is evaluated to be 152 J/mol at 720 °C and the driving force for the nucleation of austenite is 1777 J/mol for the L-Al alloy, which is quite a bit larger than that for recrystallization, which is typically 10 to ~100 J/mol.[23] Therefore, the formation of austenite in the deformed structure tends to encroach on the preferential nucleation sites for recrystallization and it also hinders the growth of recrystallized ferrite grains. Accordingly, the recrystallization will be retarded and will proceed in a sluggish manner. On the other hand, the microstructure of the cold-rolled H-Al alloy is separated into ferrite and martensite and thus the recrystallization of cold-rolled ferrite does not interfere with the austenite formation. In addition, in the region in which cold-rolled martensite exists, the competition between the recrystallization and the reverse transformation will be mitigated, because the equilibrium austenite fraction is less than that of the L-Al alloy. It suggests that the recrystallization in the H-Al alloy will proceed more effectively.

As pointed out by Matlock *et al.*, the fraction and stability of retained austenite have a significant influence on the mechanical behavior of TRIP steels.[8] Figure 5 indicates that an austenite fraction of approximately 30 pct can be obtained in both investigated alloys with appropriate annealing conditions. It has been reported that the stability of austenite depends on the grain size as well as the chemical composition.[24–26] In particular, the effect of the grain refinement becomes notable when the grain size is less than 1 μm.[24] As

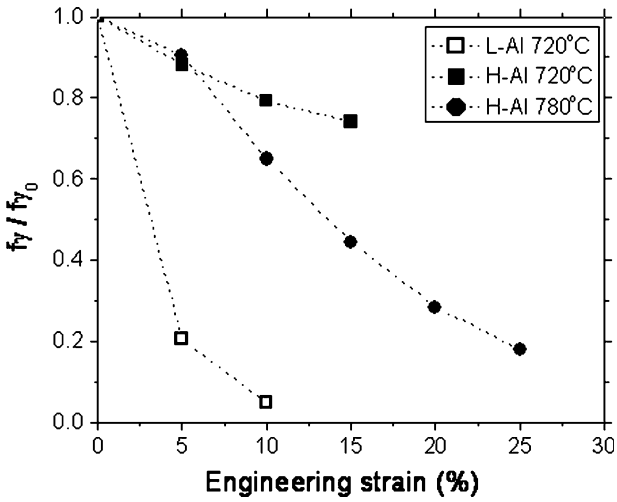

Fig. 12—Change of retained austenite fraction with apparent strain during tensile test.

mentioned, the average grain size of the austenite in the annealed sheets is far below 1 μm. Moreover, more than 90 pct of the observed austenite grains have a size below 0.5 μm, as shown in the grain size distribution given in Figure 9. Given that the M_s temperatures of the intercritical austenite calculated from the empirical equation, taking into account the chemical effect of carbon and Mn,[27] are 169 °C in the L-Al alloy annealed at 720 °C and 156 °C in the H-Al alloys annealed at 780 °C, assuming a complete redistribution of carbon into austenite, both the refinement and uniformity of the austenite grain size are thought to have a remarkable influence on the stabilization of austenite.

Figure 12 presents the change in the austenite fraction with apparent strain during the tensile test. It is noted that the austenite fraction is evaluated from the different specimen deformed to each strain. In the H-Al alloy annealed at 720 °C, only 25 pct of the initial austenite

transforms to strain-induced martensite, until the apparent strain reaches 15 pct. It implies that little work-hardening behavior in the stress-strain curve of that alloy is attributable to the stability of austenite. Considering that the austenite in the H-Al alloy annealed at 720 °C has the smallest average grain size in the present study and that more than 98 pct of the observed austenite grains are smaller than 0.5 μm, the resistance against the strain-induced transformation to martensite would originate from the fine grain size of austenite. The stress-strain curve and the change in the austenite fraction indicate that austenite stabilized more than necessary cannot provide persistent work hardening and thus becomes ineffective in preventing a local deformation, which results in deterioration in the mechanical balance. Meanwhile, the L-Al alloy annealed at 720 °C and the H-Al alloy annealed at 780 °C have similar austenite fractions and grain sizes with comparable Mn contents but show quite different tensile behaviors in Figure 11. This is associated with the dissimilar response of their retained austenite to the deformation, as shown in Figure 12. Compared with the retained austenite in the L-Al alloy, 95 pct of which transforms to martensite upon the apparent strain of 10 pct, the austenite in the H-Al alloy transforms gradually with deformation and 80 pct of the initial austenite transforms to martensite when the apparent strain becomes 25 pct, thus providing a continuous work hardening and homogeneous deformation during the tensile test. Nevertheless, it should be noted that the dissimilar response of austenite to the apparent strain does not necessarily reflect the difference in the intrinsic stability of austenite. That is because the microstructure of the annealed steels are not the same for both alloys and thus the stress or strain exerted on the austenite grain will be different even at the same apparent strain. For example, fully recrystallized ferrite matrix, as seen in the H-Al alloy, will be in charge of a considerable amount of deformation, but the lesser recrystallized matrix in the L-Al alloy will not effectively cover the deformation, and more stress or strain is possibly allocated to the austenite grains. A quantitative understanding of the different responses of austenite to the apparent strain, even with a similar morphology and chemical composition, is thought to require further investigation of a precise determination of the stress or strain allocated in the individual phase during the deformation.

VI. CONCLUSIONS

Low-carbon, manganese TRIP (Mn TRIP) steel has superior mechanical balance compared to the conventional low-carbon TRIP steels. In this study, we suggest a microstructure design based on Al additions for application of the continuous-annealing processing rather than the batch-type processing. The microstructural change after intercritical annealing and the mechanical behavior of the alloys containing 1 mass pct Al (L-Al) and 3 mass pct Al (H-Al) are investigated and following conclusions can be drawn.

1. The fraction of austenite formed during intercritical annealing can be controlled by means of Al additions to Mn TRIP steel. An Al addition of 3 mass pct limits the austenite fraction to 20 to ~30 vol pct at annealing temperatures in the range of 700 °C to ~800 °C, at which recrystallization of deformed matrix actively proceeds.
2. Appropriate annealing conditions for investigated alloys can stabilize the austenite formed during intercritical annealing. The average austenite grain size is approximately 0.22 to ~0.29 μm. In the L-Al alloy, recrystallization of the cold-rolled microstructure occurs in a sluggish manner due to the competition with the formation of austenite. Less interference between the recrystallization and the reverse transformation of the austenite allows the rapid recrystallization of the deformed structure in the H-Al alloy.
3. The austenite fraction and stability is affected by the annealing condition and the Al content. Optimization of the austenite fraction and stability in the H-Al alloy can provide an excellent mechanical balance with a tensile strength of approximately 1 GPa and a total elongation in excess of 25 pct after continuous-annealing processing.

REFERENCES

1. B.C. De Cooman: *Curr. Opin. Solid State Mater. Sci.*, 2004, vol. 8, pp. 285–303.
2. J. Bouquerel, K. Verbeken, and B.C. De Cooman: *Acta Mater.*, 2006, vol. 54, pp. 1443–56.
3. S. Zaefferer, J. Ohlert, and W. Bleck: *Acta Mater.*, 2002, vol. 52, pp. 2765–78.
4. C. Jing, D.W. Suh, C.S. Oh, Z. Wang, and S.J. Kim: *Met. Mater.-Int.*, 2007, vol. 13, pp. 13–19.
5. C.P. Scott and J. Drillet: *Scripta Mater.*, 2007, vol. 56, pp. 489–92.
6. P. J. Jacques: *Curr. Opin. Solid State Mater. Sci.*, 2004, vol. 8, pp. 259–65.
7. K. Sugimoto, M. Murata, T. Muramatsu, and Y. Mukai: *ISIJ Int.*, 2007, vol. 47, pp. 1357–62.
8. D.K. Matlock and J.G. Speer: *Proc. 3rd Int. Conf. on Advanced Structural Steels*, KIM, Gyeongjoo, Korea, 2006, pp. 744–81.
9. R.L. Miller: *Metall. Trans.*, 1972, vol. 3, pp. 905–12.
10. T. Furukawa, H. Huang, and O. Matsumura: *Mater. Sci. Technol.*, 1994, vol. 10, pp. 964–69.
11. H. Huang, O. Matsumura, and T. Furukawa: *Mater. Sci. Technol.*, 1994, vol. 10, pp. 621–26.
12. H. Takechi: *JOM*, 2008, vol. 60, pp. 22–26.
13. D.W. Suh, S.J. Park, C.S. Oh, and S.J. Kim: *Scripta Mater.*, 2007, vol. 57, pp. 1097–1100.
14. Thermo-Calc Software, Version R, *User's Guide*, Thermo-calc software AB, Stockholm, Sweden, 2007.
15. B.J. Lee: POSTECH, Pohang, Korea, private communication, 2008.
16. C.F. Jatczak: *SAE Technical Paper Series 800426*, SAE, PA, 1980, pp. 1–20.
17. B.C. Cullity: *Elements of X-Ray Diffraction*, Addison-Wesley, London, 1978, pp. 517–18.
18. "ASTM E8M-03 Standard Test Methods for Tension Testing of Metallic Materials," *Annual Book of ASTM Standards*, ASTM International, West Conshohocken, PA, 2003, vol. 03.01, pp. 1–24.
19. S.W. Thompson and P.R. Howell: *Mater. Sci. Technol.*, 1992, vol. 8, pp. 777–84.
20. D.W. Suh, S.J. Park, and S.J. Kim: *Metall. Mater. Trans. A*, 2008, vol. 39A, pp. 2015–19.
21. F. Heidelbach, H.R. Wenk, S.R. Chen, J. Pospiech, and S.I. Wright: *Mater. Sci. Eng.*, 1996, vol. A215, pp. 39–49.

22. F.J. Humphreys and M. Ferry: *Mater. Sci. Technol.*, 1997, vol. 13, pp. 85–90.
23. F.J. Humphreys and M. Hatherly: *Recrystallization and Related Annealing Phenomena*, Elsevier, Oxford, United Kingdom, 1995, pp. 8–9.
24. J. Wang and S.V.D. Zwaag: *Metall. Mater. Trans. A*, 2001, vol. 32A, pp. 1527–39.
25. D.W. Suh, S.J. Park, C.H. Lee, and S.J. Kim: *Metall. Mater. Trans. A*, 2009, vol. 40A, pp. 264–68.
26. S. Turteltaub and A.S.J. Suiker: *Int. J. Solids Struct.*, 2006, vol. 43, pp. 7322–36.
27. J. Mahieu, J. Maki, B.C. De Cooman, and S. Claessens: *Metall. Mater. Trans. A*, 2002, vol. 33A, pp. 2573–80.